Explanation of the Inverse Doppler Effect Observed in Nonlinear Transmission Lines

Alexander B. Kozyrev* and Daniel W. van der Weide

Department of Electrical and Computer Engineering, University of Wisconsin–Madison, Madison, Wisconsin 53706, USA

(Received 3 February 2005; published 23 May 2005)

The theory of the inverse Doppler effect recently observed in magnetic nonlinear transmission lines is developed. We explain the crucial role of the backward spatial harmonic in the occurrence of an inverse Doppler effect and draw analogies of the magnetic nonlinear transmission line to the backward wave oscillator.

DOI: 10.1103/PhysRevLett.94.203902 PACS numbers: 41.20.-q, 52.35.Tc, 84.40.Az, 84.40.Fe

Seddon and Bearpark (SB) reported the first observation of an inverse Doppler effect, in which the frequency of a wave is increased upon reflection from a receding boundary [1]. They used an experimental scheme based on a magnetic nonlinear transmission line (NLTL) which was suggested recently in [2,3]. This scheme falls into a general class of systems that involves the emission of phase matched high-frequency waves by an electromagnetic shock wave propagating along a NLTL with dispersion [4,5]. The moving boundary that is used to produce a Doppler shift is the discontinuity that is formed between regions of unsaturated and saturated nonlinearity in the transmission line at the leading edge of the pump pulse [1]. Under appropriate conditions, this shock wave (moving discontinuity) generates a phase matched rf wave propagating in the opposite direction to the moving discontinuity. Following its reflection from the NLTL input interface, this wave catches up with the moving discontinuity and produces an anomalous Doppler shift [3,5].

In [1] SB adopted the theory developed in [2] where the emission of a high-frequency Bloch wave by an electromagnetic shock wave phase matched with the backward spatial harmonic was discussed and the general behavior of this emission for a specific electrodynamic system having a dominant backward spatial harmonic was predicted. However, SB asserted that the shock wave generates a phase matched backward wave in the second Brillouin zone (BZ) (or ''dominating first backward spatial harmonic'' in the terminology of [2]), while their experimental setup and the model used for simulations did not allow them to track the spatial structure of the generated wave and thus make clear distinctions between a wave in the first and the second BZ. Hence, the origin and spatial structure of the emitted and reflected waves were not properly justified.

Later, Reed *et al.* criticized the theory used in [1] and the interpretation of the measured results, and proposed an alternative explanation of the observed effect [6]. They applied a theoretical framework for describing the reflection of an electromagnetic wave from a moving shock like discontinuity induced in photonic crystals [7] to explain the anomalous Doppler shift reported in [1]. They considered waves in the second BZ in the system studied in [1] to be unphysical, and assumed that the shock wave front emits the waves in the first BZ with the same frequency. Furthermore, they connected the observed effect with a periodic dependence of the reflection coefficient, which would introduce an additional phase shift term at the moving boundary and lead to the anomalous Doppler shift.

Here we present the results of an analytical study and simulations of the spatial structure of the wave excited by the shock wave discontinuity, and thus overcome the discrepancy between SB and Reed *et al.* We prove that the existence of backward spatial harmonics is crucial for the observed inverse Doppler effect in magnetic NLTLs. We also discuss the physical processes arising at the nonlinear interaction of a shock wave and an rf wave which lead to the inverse Doppler shift and justify the analogy of this system with a backward wave oscillator (BWO).

In order to clarify the origin of the wave emitted by a shock wave, together with the mechanism of the anomalous Doppler shift after its reflection from the moving discontinuity, we need to trace the spatial structure of the waves propagating along the NLTL with capacitance cross-links. The model considered in [1] [an *LC* circuit with capacitance cross-links shown in Fig. 1(a)] does not allow us to distinguish a particular spatial harmonic due to the discrete nature of the model. The circuit model shown in Fig. 1(b), where each *LC* section is replaced with the

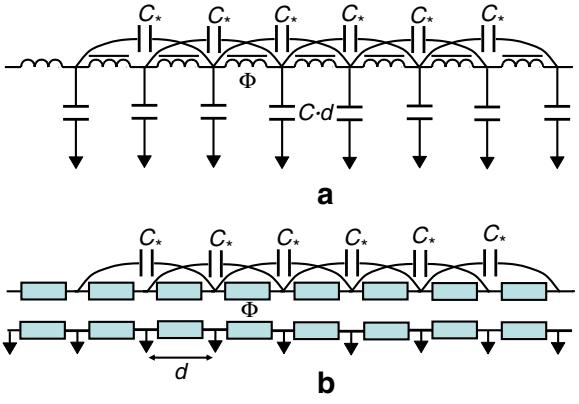

FIG. 1 (color online). Equivalent circuit of (a) discrete *LC* circuit with capacitive cross-links and (b) distributed NLTL with capacitive cross-links.

 © 2005 The American Physical Society

length of NLTL, should be used instead. The medium behind the shock wave front saturates and becomes linear [4]; therefore the system shown in Fig. 1(b) is a periodically loaded distributed transmission line which supports Bloch waves [8],

$$V_B(z) = V_p e^{-j\beta z} = V^+ e^{-jk_0 z} + V^- e^{jk_0 z}, \quad (1)$$

where V_p is a periodic function with period d, β is the propagation constant of the periodic structure, k_0 is the propagation constant in unloaded transmission line, and

$$V^- = -V^+(1 - e^{-jk_0 d + j\beta d})/(1 - e^{jk_0 d + j\beta d}). \quad (2)$$

Bloch waves can be expanded into an infinite set of spatial harmonics so that the field in a periodic structure can be represented as

$$V_B = \sum_{n=-\infty}^{n=\infty} V_{p,n} e^{-j\beta_n z}. \quad (3)$$

Each term in this expansion is a spatial harmonic, is periodic in spatial amplitude $V_{p,n}(z + d) = V_{p,n}(z)$, and has propagation phase constant $\beta_n = \beta + 2n\pi/d$. All harmonics propagate with the same group velocity; however, some of the spatial harmonics have phase and group velocities that are oppositely directed (backward spatial harmonics) since β_n can be both positive and negative. The dispersion equation for the saturated transmission line relating β and k_0 is

$$\cos\beta d - \cos k_0 d + 2\gamma_* k_0 d \sin k_0 d \sin^2 \beta d = 0. \quad (4)$$

Figure 2 shows the $k_0 d - \beta d$ diagram for $\gamma_* = C_*/Cd = 1.124$ (C_* is the cross-link capacitance and C is the line capacitance per unit length), which corresponds to the system described in [1]. Coefficients in the expansion (3) (or amplitudes of spatial harmonics) for the system shown in Fig. 1(b) can be calculated with (2) and (4), as described in [8]. Figure 3 shows the dependence of the ratio of the amplitude of the first backward spatial harmonic to the amplitude of the zeroth spatial harmonic on the propagation constant β for different values of γ_*. Each has a pronounced maximum at some value of β and the ratio increases with γ_*. In the case of the system realized in [1] $\gamma_* = 1.124$ and the maximum value of the ratio $|V_{p,-1}|/|V_{p,0}|$ is 0.45. This means that, although the first backward spatial harmonic is not dominant like it was assumed in [1], it does have a relatively large amplitude and can not be simply excluded from consideration, as was suggested in [6].

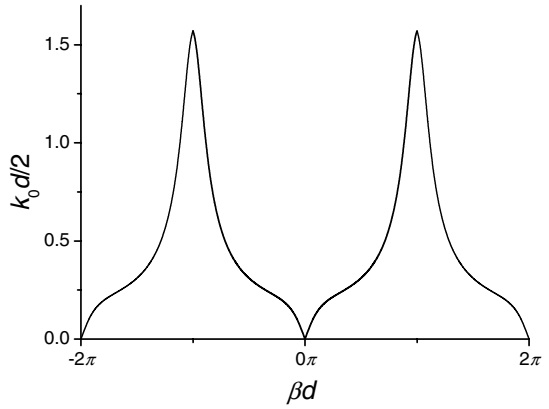

FIG. 2. $k_0 d - \beta d$ diagram of the distributed NLTL with capacitance cross-links shown in Fig. 1(b) for $\gamma_* = 1.124$.

Our transient time-domain simulations confirm that the real physical mechanism responsible for the observed inverse Doppler shift is more complicated than the interpretation given by SB and Reed *et al.* We modeled each length of the distributed NLTL in Fig. 1(b) using n sections of LC networks composed of series nonlinear inductances having saturated values Ld/n (L is the inductance per unit length for saturated nonlinearity) and parallel capacitances Cd/n so that the capacitive cross coupling would be through $2n$ sections (instead of two like in [1]). In our simulations $n = 100$, and they used parameters specified in [1].

Figure 4 shows the spectrum of the voltage waveform at the 30th section of the magnetic NLTL [$v_s/v_0 = 0.285$, v_s is the shock wave velocity, and $v_0 = 1/(LC)^{1/2}$]. There are three distinct peaks: the low-frequency one corresponds to the Bloch wave emitted by the shock wave. The first backward spatial harmonic of this wave is phase matched with the shock wave discontinuity so that $v_s = \omega/(\beta + 2\pi/d)$ ($\beta \approx -0.75\pi$). After being emitted, this wave "1" propagates in the direction opposite to the discontinuity and is reflected from the input terminal of the NLTL as a wave "1′", which propagates in the same direction as the discontinuity. Wave "1′" is a simple reflection of wave "1"; the frequency ω_1 and group velocity for waves "1" and "1′" are equal, but their directions are reversed by the reflection. The dispersion characteristics are designed such that the magnitude of the group velocity for waves "1" and "1′" is greater than the velocity of the discontinuity (Fig. 4), so wave "1′" catches up to the discontinuity and is reflected from it to produce a Doppler up-shifted

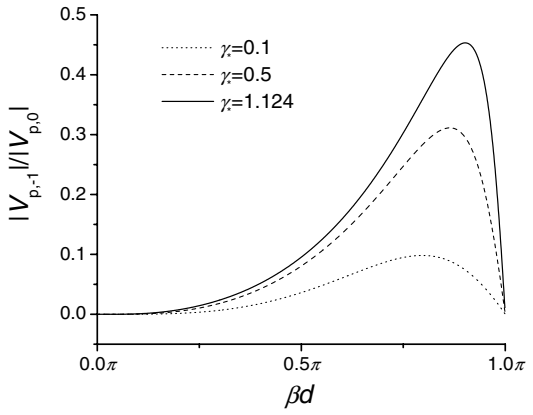

FIG. 3. The dependence of the ratio of the amplitude of the first backward spatial harmonic to the amplitude of the zeroth spatial harmonic on the propagation constant β for different values of parameter γ_*.

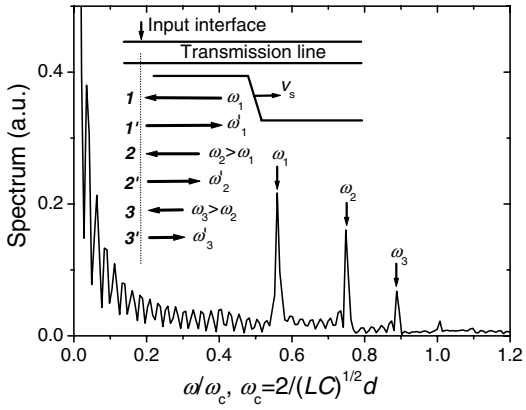

FIG. 4. The spectrum of the voltage waveform at the 30th section of the magnetic NLTL.

Bloch wave "2" (with frequency ω_2). Depending on the dispersion characteristic of the system, there can be several subsequent reflections. For the parameters here, the dispersion of the system is such that the direction of wave "2" is opposite to the direction of shock wave propagation and its group velocity is higher than the shock wave velocity. Thus, wave "2" after reflection from the input interface will catch up to the moving discontinuity again and will reflect back with an increase of frequency, giving rise to wave "3" (with frequency ω_3).

Figure 5 shows the space-domain spectrum (Fourier transform) of the instantaneous voltage distribution along the NLTL. Peak $\beta_{1,0}$ in the first BZ ($0 \le |\beta d| \le \pi$) and peak $\beta_{1,1} = 2\pi/d - \beta_{1,0}$ in the second BZ ($\pi \le |\beta d| \le 2\pi$) can be easily identified as absolute values of the zeroth forward and first backward spatial harmonics of the Bloch wave having frequency ω_1. (Values $\beta_{1,0}$ and $\beta_{1,1}$ are the absolute values due to the fact that a FFT does not distinguish between the positive and negative phase constants. The wave emitted by a shock wave propagating in the positive direction has a negative phase constant for the zeroth spatial harmonic and a positive one for the first backward spatial harmonic.) Thus, in distinction to SB

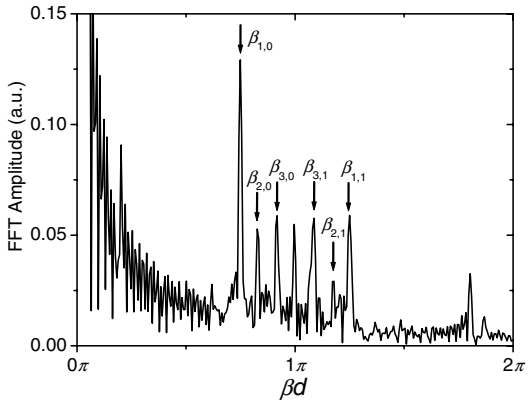

FIG. 5. The space-domain spectrum (FTT transformation) of the instantaneous snap of the voltage distribution along the NLTL at $t/\tau_0 = 439$ [$\tau_0 = 1/d(LC)^{1/2}$].

[1] and Reed *et al.* [6], who assumed that the shock wave emits either a wave with $\beta_{1,1}$ or a wave with $-\beta_{1,0}$, our simulations show that the shock wave propagating in a magnetic NLTL having capacitive cross-links emits a Bloch wave with both zeroth and first backward spatial harmonics. Higher spatial harmonics are also present, but their amplitudes are negligible. In a similar manner, peaks $\beta_{2,0}$ and $\beta_{2,1} = 2\pi/d - \beta_{2,0}$, as well as $\beta_{3,0}$ and $\beta_{3,1} = 2\pi/d - \beta_{3,0}$, can be identified as absolute values of the zeroth and the first backward spatial harmonics of the Bloch waves having frequencies ω_2 and ω_3, respectively.

The excitation efficiency of the Bloch wave by the shock wave when the latter is phase matched with the first spatial harmonic depends on the relative amplitude of the first spatial harmonic in the wave. If the amplitude of the first spatial harmonic is small compared to the amplitude of the zeroth spatial harmonic, then the Bloch wave cannot be effectively excited. Experimental data described in [1] correspond to the range where this ratio is at a maximum. This explains the excitation of the Bloch wave by the shock wave in our simulations, as well as the existence of spatial periods falling into the second BZ. Thus, the simulations prove that the mechanism for the emission of high-frequency waves is essentially the same as in the BWO (as it was suggested in [2,9]).

Physical phenomena that occur when rf electromagnetic waves reflect from an electromagnetic shock wave front propagating along a periodic magnetic NLTL can be understood by considering the boundary condition for the electromagnetic field at the shock wave discontinuity. The electromagnetic shock wave is a nonlinear region where a sharp transition between two states of the medium takes place. Here we have a moving boundary between unsaturated and saturated states of the ferrite-filled magnetic NLTL, and the boundary condition connecting parameters of the medium before and after the transition, as described in [10]:

$$\{I - \nu_s CV\} = \{V - \nu_s \Phi(I)\} = 0, \tag{5}$$

where I, V, and Φ stand for the magnitudes of current, voltage, and magnetic flux before and after the discontinuity. The interaction of a small-signal rf wave with an intensive electromagnetic shock wave has already been discussed in the literature [11,12]. The general condition for shock wave stability in the presence of perturbations requires that only the reflected wave (or waves, if dispersion permits) may exist; no transmitted rf waves can be generated. In this case there are two boundary conditions (5) and only one unknown, the amplitude of the reflected wave. To obtain a unique, finite solution, one must note the effect of the incident wave on the motion of the shock front and consider the perturbation of the shock wave velocity. From (5), the velocity of the shock discontinuity is determined by the values of current, voltage, and magnetic flux before and after the discontinuity. The voltage and the current drops across the discontinuity are

$$V_{12} = V_s + V_{B1} + V_{B2}, \quad (6)$$

$$I_{12} = I_s + I_{B1} + I_{B2} = \frac{V_s}{\nu_{s0}C} + \frac{V_{B1}}{Z_{B1}} + \frac{V_{B2}}{Z_{B2}}, \quad (7)$$

where V_s and I_s are the unperturbed values of the shock wave current and the voltage, while V_{B1}, I_{B1}, Z_{B1} and V_{B2}, I_{B2}, Z_{B2} are, respectively, the voltage, current, and the impedance of the incident and the reflected Bloch waves. Assuming that the discontinuity velocity affected by the presence of an incident and a reflected wave can be expressed as

$$\nu_s = \nu_{s0} + \delta\nu_s, \quad (8)$$

where ν_{s0} is the unperturbed value of the shock wave velocity in the absence of incident wave, and $\delta\nu_s$ is the velocity perturbation due to the interaction with the incident wave. Taking into account (6) and (7), the boundary condition can be transformed to

$$I_{12} - \nu_{s0}CV_{12} - \delta\nu_s CV_s = V_{12} - \nu_{s0}\Phi_{12} - \delta\nu_s\Phi_0 = 0. \quad (9)$$

Here Φ_{12} and Φ_0 are the perturbed and unperturbed magnetic flux change across the shock wave discontinuity. Thus, the relative amplitude of the reflected wave can be estimated as

$$\frac{V_{B2}(z)}{V_{B1}(z)} = \frac{(\nu_s L + 1/C\nu_s)/Z_{B1} - 2}{2 - (\nu_s L + 1/C\nu_s)/Z_{B2}}. \quad (10)$$

The frequency of the reflected wave can be obtained from the phase continuity condition at the shock wave front

$$\omega_1 - \beta_1\nu_s = \omega_2 - \beta_2\nu_s + 2\pi m/d. \quad (11)$$

Here ω_1, β_1 and ω_2, β_2 are the frequencies and propagation phase constants for the incident and reflected waves, respectively, and m is an integer value. The last term in (11) is connected with the spatial periodicity of the Bloch wave. The amplitudes, frequencies, and wave numbers predicted by (10) and (11) are in good agreement with the results of our simulations.

Reed *et al.* [6] claimed that the system used to observe inverse Doppler effect in [1] ''falls into the general class of systems that involve a propagating shock like excitation in a periodic system, where they predicted an inverse Doppler effect using a different theoretical framework.'' They suggested using this theoretical framework to explain the inverse Doppler effect reported in [1]. Though systems described in [1,7,13] indeed look very similar, the physical processes that lead to the anomalous effect are still fundamentally different. In the shocked photonic crystals studied in [7], the shocklike excitation is produced externally and the shock wave velocity is not affected by the incident electromagnetic field. There is no nonlinear interaction between the shock wave and the incident electromagnetic wave, and the latter is reflected from the boundary between media having different dielectric constants. In this case, two incident waves produce both reflected and transmitted waves, although the transmitted wave is evanescent. In the theoretical framework used in [7], this is taken into account introducing a space dependent reflection coefficient, which is well justified. This reflection coefficient was assumed to be a periodic function in space due to the intrinsic periodicity of a photonic crystal. However, the formal introduction of the space dependent reflection coefficient suggested in [6] to explain the inverse Doppler shift observed by SB has no physical basis, since there is no transmitted wave in the region before the *electromagnetic* shock wave discontinuity according to the shock wave stability condition. Thus, although the theoretical framework described in [6] correctly describes anomalous effects at the propagation of the shocklike mechanical excitations in periodic photonic crystals, its conclusions cannot be directly applied to the system suggested in [2] and realized in [1] due to fundamental differences between the systems.

The improved distributed model of the system studied in [1] allowed us to prove the crucial role of the first backward spatial harmonic which is phase matched with shock wave discontinuity propagating along magnetic NLTL for emission of the rf wave, as well as to explain the occurrence of the inverse Doppler effect. The results of our simulations, together with the analysis of the physical phenomena at the shock wave discontinuity, enable us to overcome discrepancies between the previously suggested interpretations of the observed inverse Doppler effect as given in [1,6].

We thank N. Seddon and A. M. Belyantsev for discussions on NLTLs. This work was supported by the Air Force Office of Scientific Research under the Multidisciplinary University Research Initiative Grant No. F49620-03-1-0420.

*Electronic address: abkozyrev@wisc.edu

[1] N. Seddon and T. Bearpark, Science **302**, 1537 (2003).
[2] A. M. Belyantsev and A. B. Kozyrev, Tech. Phys. **45**, 747 (2000).
[3] A. M. Belyantsev and A. B. Kozyrev, Tech. Phys. **47**, 1477 (2002).
[4] A. M. Belyantsev and A. B. Kozyrev, Tech. Phys. **43**, 80 (1998).
[5] A. M. Belyantsev and A. B. Kozyrev, Mater. Sci. Forum **297–298**, 349 (1999).
[6] E. J. Reed, M. Soljacic, M. Ibanescu, and J. D. Joannopoulos, Science **305**, 778b (2004).
[7] E. J. Reed, M. Soljacic, and J. D. Joannopoulos, Phys. Rev. Lett. **91**, 133901 (2003).
[8] R. E. Collin, *Foundations for Microwave Engineering* (McGraw-Hill, Inc., New York, 1992), 2nd ed.
[9] N. Seddon and T. Bearpark, Science **305**, 778c (2004).
[10] A. V. Gaponov, L. A. Ostrovskii, and G. I. Freidman, Radiophys. Quantum Electron. **10**, 772 (1967).
[11] L. A. Ostrovskii and N. S. Stepanov, Radiophys. Quantum Electron. **14**, 387 (1971).
[12] L. A. Ostrovskii, Sov. Phys. Usp. **18**, 452 (1975).
[13] E. J. Reed, M. Soljacic, and J. D. Joannopoulos, Phys. Rev. Lett. **90**, 203904 (2003).